AIAA Journal A Publication of the American Institute of Aeronautics and Astronautics

VOLUME 1 NOVEMBER 1963 NUMBER 11

Drag of Spheres in Rarefied Hypervelocity Flow

MAX KINSLOW* AND J. LEITH POTTER†
ARO Inc., Arnold Air Force Station, Tenn.

Drag of spheres has been measured under hypersonic, cold-wall, support-free conditions in a nonreacting flow in which molecular vibration was frozen. Data were obtained for a nominal freestream Mach number of 11 and for Reynolds numbers from 1 to 10 based on conditions immediately downstream of the normal shock and sphere diameter. These data were supplemented by measurements at a nominal Mach number of 10 where a conventional balance was used, and Reynolds numbers downstream of the shock as high as 10^4 were investigated in the cold-wall condition. The experimental results have been analyzed both from the viewpoint of continuum flow with second-order viscous effects and from the standpoint of a noncontinuum concept, taking account of first collisions between re-emitted and freestream molecules. In both cases, useful, semiempirical expressions for drag coefficient are derived. The first-collision analysis is numerically indeterminant because of the lack of a method for explicit calculation of mean free path. However, the form of the derived equation for drag coefficient in noncontinuum flow is particularly suitable for modification to permit its use in linking free-molecule solutions and available experimental data. This possibility is suggested because the limiting drag coefficient at high Reynolds numbers is on the order of the accepted value for continuum, inviscid flow.

Nomenclature

A = $[(r/\lambda)^2 - (R/\lambda)^2]^{1/2}$
a = speed of sound $(\gamma RT)^{1/2}$
B = $r/\lambda - R/\lambda$
C = empirical factor
C_D = drag coefficient, defined by Eq. (1)
C_{Dfm} = free-molecule drag coefficient
C_{Di} = inviscid drag coefficient
d = diameter of sphere
dA = elemental area of surface
$d\omega$ = incremental solid angle
$-Ei(-x)$ = generalized exponential integral, $\int_x^\infty (e^{-x}/x)dx$
H_w = enthalpy parameter, $H_w = h_w/h_0 - 1$
h = enthalpy
K_1, K_2 = coefficients
Kn = Knudsen number
k = Boltzmann constant
l = coordinate measured from a point on a surface to a point in space
M = Mach number
m = mass of a molecule
N = number flux of molecules
n = number density of molecules
$n(v)$ = number density of molecules in velocity, position coordinates
R = radius of sphere
$\Re$ = gas constant, k/m
Re = Reynolds number, $Ud\rho/\mu$
r = coordinate from center of sphere (see Fig. 9)
S = molecular speed ratio, $U/(2\Re T)^{1/2}$
T = temperature
U = velocity
v = velocity of a molecule
x = axial coordinate
γ = ratio of specific heats
Δx = difference between axial coordinates
η = collision rate density between wall and freestream molecules
θ = angle between normal to dA and the freestream velocity vector (see Fig. 8)
λ = mean free path
μ = viscosity
ρ = mass density
ϕ = angle between the normal to dA and the velocity vector of a reemitted molecule (see Fig. 8)

Subscripts

0 = total or isentropic stagnation condition
2 = condition immediately downstream of normal shock
i = incident molecules
s = scattered molecules
w = wall condition
∞ = freestream condition

Received January 16, 1963; revision received July 22, 1963. This work has been sponsored by the Arnold Engineering Development Center, Air Force Systems Command, U. S. Air Force, under Contract No. AF40(600)-1000, Air Force Systems Command Program Area 750A, Project 8953, Task 895306.

* Research Engineer, Research Branch, von Kármán Gas Dynamics Facility, Arnold Engineering Development Center.

† Manager, Research Branch, von Kármán Gas Dynamics Facility, Arnold Engineering Development Center. Associate Fellow Member AIAA.

Introduction

THE drag coefficients of hypersonic spheres at both very high Knudsen numbers (>10) and very low Knudsen numbers ($<10^{-4}$) are known to at least a moderate degree of accuracy, although there is uncertainty regarding the accommodation coefficients in free-molecular flows. In the intermediate range of Knudsen numbers, where neither analysis nor experiment has fully answered the question, significant contributions have been made by both approaches.[1-16]

With regard to the high Knudsen number or near-free-molecular flow regime, the obstacles to analytical solution arise chiefly from the lack of exact knowledge of the behavior of

molecules after impact on the sphere and the mathematical complexity of the flow model when interactions between free-stream and reflected molecules become important. In the continuum, viscous-interaction regime of small Knudsen numbers, the usual difficulty of dealing with flows characterized by thick boundary layers in the presence of vorticity, curvature, displacement, slip, and temperature jump presents the main obstacle.

The reason that experimental data have not been presented for the entire intermediate regime is basically the lack of facilities capable of duplicating all the conditions of flow desired for the investigation. Nonetheless, experimental data provide the more significant part of the knowledge of sphere drag in the region $10^{-4} < Kn_\infty < 10$, where Kn_∞ is based on free-stream conditions and sphere diameter.

The low-density, hypervelocity (LDH) wind tunnel of the von Kármán Gas Dynamics Facility, Arnold Engineering Development Center, Air Force Systems Command has been used to extend previous experimental studies of drag of spheres in low-density flow. Using the LDH tunnel, drag data have been taken under hypersonic, cold-wall ($T_w \ll T_0$) support-free conditions that are described later.

These and earlier data from other sources have been examined in regard to both continuum and noncontinuum fluid flow behavior. The purpose of this paper is to present the new data and analyses.

Experimental Procedure and Data

LDH Wind Tunnel

The LDH tunnel[7,17,18] is of the continuous type, with the gas heated by an electric arc or plasma generator. Test section conditions have been determined from analysis of impact pressure, local mass flow rate, calorimeter, and static pressure measurements. Briefly, the tunnel consists of a d.c. arc-heater, relatively large stilling chamber, conical nozzle of 15° half-angle and 6-in. diam exit, test chamber with instrumentation, diffuser, and pumping system.

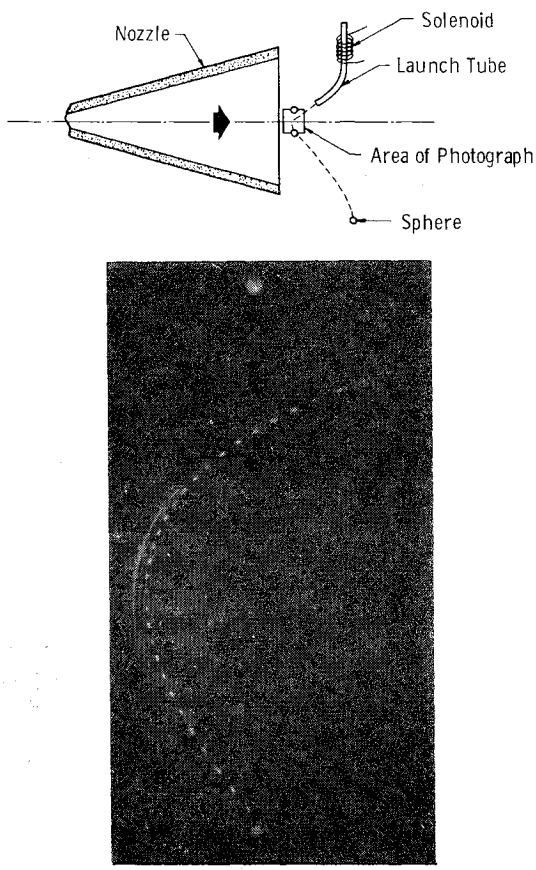

Fig. 1 Typical trajectory of sphere during free flight through test section.

Measurements of total enthalpy at the nozzle throat by calorimetry agree closely with total enthalpy computed on the basis of measured mass flow rate, total pressure, sonic throat area, and the assumption of thermodynamic equilibrium in the fluid upstream of the throat. However, on the basis that computed relaxation lengths for molecular vibration downstream from the throat are from 10^2 to 10^4 times the local nozzle radius, all theoretical evidence indicates frozen flow from the throat onward. Thus, test section flow characteristics are based on sudden freezing of molecular vibration at the throat. Operating conditions for this experiment are shown in Table 1.

Table 1 Operating conditions

Gas	Nitrogen			
Nominal nozzle station	1.0 in. downstream of exit			
Dynamic pressure, psfa	2.12	2.51	3.16	3.31
Total enthalpy, Btu/lb	871	1110	1560	1760
Total temperature, °R	3150	3960	5400	6030
Mach number	10.8	10.6	10.7	10.6
Unit Re_∞/in.	466	426	344	301
Unit Re_2/in.	47.0	42.6	37.6	34.7
Mean free path λ_∞, in.[a]	0.0342	0.0370	0.0462	0.0523

[a] Using $\lambda_\infty = 1.26\,\gamma^{1/2}\,\mu_\infty/(\rho_\infty\, a_\infty)$.

Sphere Drag Measurement

Free-fall method

For the smaller spheres (0.0313- to 0.375-in. diam), a free-fall technique was used to determine drag. The models were injected into the test stream and their trajectories determined using a photographic technique whereby a time exposure was made of the moving model, which was illuminated by an interrupted light source. Spheres with diameters of 0.0625 to 0.375 in. were dropped into the test section by an electromagnet from a position just above the test section. However, the spheres had a tendency to retain some residual magnetism, thereby making release of the smaller spheres difficult. In order to facilitate the release of the smaller spheres, a solenoid was wound near the end of a short length of copper tubing. With the solenoid energized, spheres of 0.0313- to 0.156-in. diam could be suspended within the tubing. By de-energizing the solenoid, the models were free to fall down the tubing. The end of the tubing was bent so that the models could be injected into the test stream at the appropriate angle.

The light source used to illuminate the spheres during their flight through the test section was a 1000-w projector lamp. The light intensity was modulated using a rotating disk containing holes drilled around the periphery. The disk was rotated by a high-speed motor so that the light at the test section could be interrupted at rates up to 1000/sec. By taking a time exposure of the test section, the trajectory of the sphere was recorded photographically at equal time intervals during its flight.

Since the usable test section is about 1 in. in diameter, a telephoto lens was used so that the photograph of the test region could be magnified for easier data reduction. An example is shown in Fig. 1.

Surface temperatures of the spheres tested by the free-flight method were approximately 0.1 total temperature.

Axial-force balance

A small amount of data was obtained earlier for spheres of 0.265- to 0.686-in. diam by means of an external, sting-type, water-cooled, axial-force balance capable of measuring forces on the order of 0.001 lb. Temperatures of the spheres on this balance were somewhat greater than in the free-fall case,

although $T_w < T_0$, and minimum sphere size was limited to approximately 0.25 in.

The test spheres were steel ball bearings with a 0.1-in. hole drilled to admit the sting support. The spheres were uncooled except for radiation from the surface and conduction through the sting mount. Wall temperature of the spheres reached approximately 0.3 total temperature.

It should be noted that the data obtained by the balance were published previously,[7] but the points now have been shifted slightly because of the use of a new source of viscosity of nitrogen at high temperatures.[19] Good agreement is evident in comparing free-fall and balance measurements.

A small quantity of new data at higher Reynolds numbers from the 50-in. Mach 10 tunnel C in the von Kármán Facility is included. These were obtained by use of the same axial-force balance used in the LDH tunnel.

Data Reduction

The data from the free-fall tests were obtained in the form of photographs (Fig. 1) that showed the trajectory of the sphere at equal time increments. One exposure was made of the path of the sphere and the other of two reference light sources that could be positioned on the nozzle exit before or after a run.

The difference in axial coordinates of adjacent points, Δx, was plotted as shown in Fig. 2. The slope of the line through these points is proportional to the acceleration of the sphere in the axial direction. The constant of proportionality between this slope and the sphere acceleration was obtained by combining the known time between successive points on the photograph and the known scale factor of the photograph. The choice was made to combine the time and position scales into one constant so that graph paper could be used to read coordinates, and the points could be plotted simply as a function of point number. It can be shown that this finite difference method for obtaining the acceleration of a model in a uniform force field gives a result equal to that from the second derivative of the position-time curve.

Using Newton's second law, the total drag force on a sphere was determined from its acceleration and its mass. The mass was determined by using an analytical balance for weighing several spheres of the same size and then taking an average. Values of the drag coefficient C_D were obtained for the spheres using the definition

$$C_D = 2D/(\rho_\infty U_\infty^2 \pi R^2) \quad (1)$$

where D is the drag of the sphere.

Reduction of data from the axial-force balance was accomplished by the usual, well-known procedure involving use of a calibration curve obtained by static calibration of the balance using known drag loads.

Analysis

The Sphere in Low-Density, Continuum Flow

It is a generally accepted approximation that the drag coefficient of a sphere in supersonic, low-density but continuum flow may be expressed as the sum of its drag coefficient at essentially infinite Reynolds number C_{D_i}, plus the contribution from skin friction, plus a third term representing the combined influences of vorticity, slip, temperature jump, curvature, and displacement (cf., Refs. 11 and 20–23). Following from this concept, one is led to write

$$C_D = C_{D_i} + K_1(Re_2)^{-1/2} + K_2(Re_2)^{-1} + \ldots \quad (2)$$

This is the form indicated by Aroesty[16] in discussing the subject, and it is interesting to note his comment that neither the sign nor magnitude of K_2 has been established previously.

A presentation of both the new and the more recent of the previously published measurements of drag of spheres in supersonic and hypersonic flows is given in Figs. 3–5, where Re_2 is used as the parameter. (The conventional Rankine-Hougoniot shock wave is hereafter assumed in computing Re_2, and the sphere diameter is used as the characteristic length.) Curves of the form described by Eq. (2) have been fitted to these data, with C_{D_i} taken from Ref. 24 for corresponding Mach numbers. The values of K_1 and K_2 determined by this process are presented in Figs. 6 and 7 as functions of the enthalpy parameter H_w because the heat-transfer situation would be expected to be important. However, it is apparent that Mach number or some function thereof exerts an influence on the coefficients.

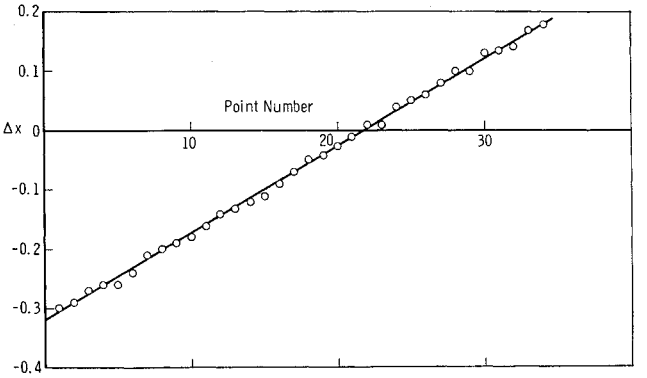

Fig. 2 Axial displacement of spheres as a function of data point number.

Although there is the possibility of correlating K_1 and K_2 with known parameters, it must be remembered that base drag could be important at the lower Mach numbers.[25, 26] In view of this, plots of the coefficients as functions of Mach number or density ratio may not be unique for $M_\infty \gtrsim 6$. Therefore, no additional correlations are presented. There is evidence in Figs. 6 and 7 that K_1 and K_2 tend toward dependence on H_w alone at large Mach numbers in the essentially perfect gases represented.

It is thought that the more conclusive portions of Figs. 6 and 7 are those pertaining to the cold-wall, hypersonic case because the influence of base pressure and other Mach-number-dependent factors must be minimized there. Also, variations about the nominal Mach number in the experiments would have less effect on the data, thereby decreasing scatter and aiding in determining the coefficients.

The situation is less clear in regard to K_2 because it assumes importance only at the lowest Reynolds numbers, and some older data do not penetrate sufficiently into that regime. The values of K_2 deduced from the data are consistently negative.

It is important to keep in mind that Eq. (2) must fail at sufficiently low Reynolds numbers. This failure may be postponed by inserting additional terms, but that is not possible in the absence of reliable drag data for very nearly free-molecular flow. Finding the subsequent terms does not seem to be highly important in the cold-wall, hypersonic case since the two terms identified here are sufficient to the limit of continuum flow, where it is then necessary to seek further extensions by means of noncontinuum flow analysis.

Aerodynamic Drag in Near-Free-Molecular Flow

Two analytical methods have been attempted for the near-free-molecule flow regime. One of these is an intuitive approach wherein the effects of collisions between molecules emitted from the body and freestream molecules are considered. This is the so-called first-collision method. The other approach is an attempt to approximate the solution of the Boltzmann equation for a body in near-free-molecule flow. Among the noteworthy investigations are those of Baker and Charwat,[9] who followed the first-collision method, and that

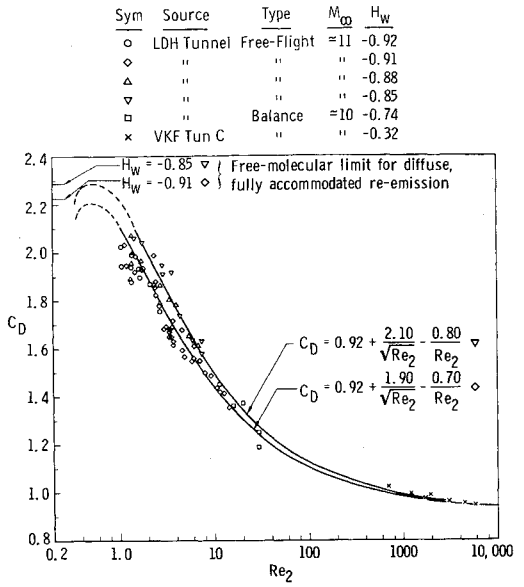

Fig. 3 Drag of spheres in hypersonic flow with $h_w < h_0$: new data.

of Willis,[10] who obtained an iterative solution of the Boltzmann equation. A semiempirical method for the transitional region has been proposed by Rott and Whittenbury.[11] The results of these three theories are compared later with the equation developed in this paper.

In the near-free-molecular flow regime, the number of freestream molecules striking the surface is diminished from the free-molecular value because some have been deflected by molecules reemitted from the body. In order to facilitate a discussion of molecular collisions, velocity distribution, and other properties of molecules, it is desirable to divide the molecules into various classes according to their past history. The undisturbed medium through which the body is moving is identified by the subscript ∞. Molecules that have been reflected from the wall and have not experienced a collision with molecules of a different class are given the subscript w. Molecules that actually strike the surface are known as incident molecules and are given the subscript i. In the near-free-molecule region, it will be assumed that the incident molecules are composed of molecules from the freestream which have not undergone a collision with molecules emitted from the wall prior to impacting upon the surface. Freestream molecules and molecules from the wall which collide with each other are shifted into the class of scattered molecules and are given the subscript s.

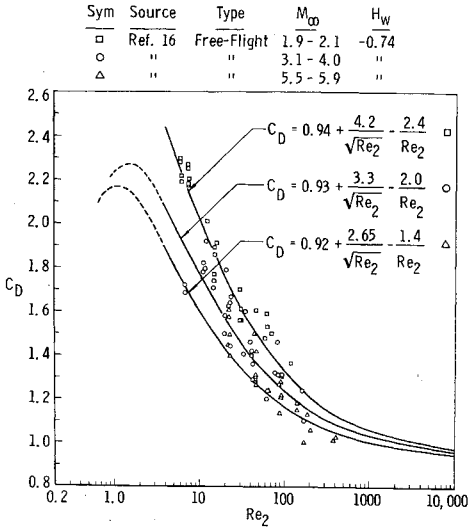

Fig. 4 Drag of spheres in supersonic flow with $h_w < h_0$.

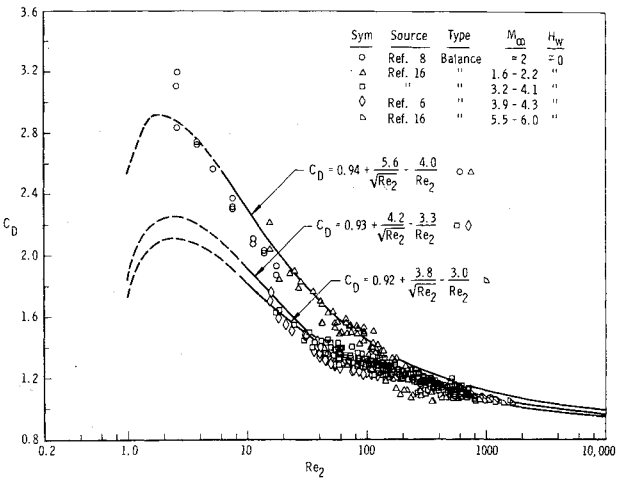

Fig. 5 Drag of spheres in supersonic flow with $h_w \simeq h_0$.

In the near-free-molecule flow analysis that follows, it is assumed that a freestream molecule is put in the scattered class only by a collision with a molecule from the wall, and that scattered molecules do not contribute to the drag of the sphere. In other words, the shielding effect of the molecules emitted from the sphere is the only effect considered.

By determining the relative number of collisions per unit time between freestream molecules and molecules re-emitted from the wall, the number of freestream molecules that become incident molecules can be found. If it is assumed that incident molecules are composed only of freestream molecules that have not experienced a collision, the drag coefficient of the sphere is simply

$$C_D = C_{Dfm}(n_i/n_\infty) \tag{3}$$

in the near-free-molecule regime.

The number of molecules incident upon an elemental area dA per unit time for large speed ratio S is[27] (see Nomenclature and Fig. 8)

$$n_i[(kT_i)/(2m)]^{1/2}2S\cos\theta dA \tag{4}$$

In the case of diffuse reflection from a surface, it is assumed here that the reflection from each incremental surface area is the same as the effusive flow of a hypothetical gas at wall temperature through an opening replacing the incremental area. The number density n_w of this hypothetical gas can be determined on the basis of the conservation of molecules.

From Kennard,[28] the number of molecules crossing any incremental area within a gas per unit time with speeds between v and $v + dv$ within the solid angle $d\omega$ is

$$n(v)dv = n_w(m/2\pi kT_w)^{3/2}v^3 \exp(-mv^2/2kT_w)\cos\phi dv d\omega dA$$

Integrating over all speeds, the total number flux of molecules, N, passing (re-emitted from) dA within the solid angle $d\omega$ is

$$N = n_w(2kT_w/m)^{1/2}(2\pi^{3/2})^{-1}\cos\phi d\omega dA \tag{5}$$

Because it is assumed that the flow is reflected symmetrically about the normal to the surface, $d\omega$ may be written as (see Fig. 8)

$$d\omega = 2\pi\sin\phi d\phi \tag{6}$$

The total number flux of molecules within the incremental angle $d\phi$ is, substituting Eq. (6) in Eq. (5),

$$n_w(2kT_w/m)^{1/2}\pi^{-1/2}\cos\phi\sin\phi d\phi dA \tag{7}$$

Integrating (7) over all directions in which molecules can be reflected from the surface ($0 \leq \phi \leq \pi/2$) gives the total number flux of molecules reflected from the surface:

$$n_w(2kT_w/\pi m)^{1/2}(dA/2) \tag{8}$$

Equating this expression to the number of incident molecules gives a solution for the number density n_w:

$$n_w = n_i(T_i/T_w)^{1/2}2\pi^{1/2}S\cos\theta \tag{9}$$

Consider the molecules leaving a surface dA within a solid angle $d\omega$. These molecules will remain within this solid angle until they undergo a collision with another molecule. The number flux of the molecules reflected from the surface and reaching a distance l without undergoing a collision may be calculated by applying a relation given by Present:[29]

$$N(l) = N(0)\exp(-l/\lambda) \tag{10}$$

The mean free path λ in Eq. (10) is the mean distance from the body to the first collision between a re-emitted molecule and a molecule of another class.

Differentiating Eq. (10) and multiplying by dl gives the number of collisions between l and $l + dl$. Using Eq. (5) with $N = N(0)$ and dividing by the incremental volume $l^2d\omega dl$ gives the number of collisions per unit volume per unit time at a point in space involving molecules that emanate from a surface element dA [The number density n_w is given by Eq. (9)]:

$$d\eta = n_w(2kT_w/m)^{1/2}\cos\phi\exp(-l/\lambda)dA/(2\pi^{3/2}\lambda l^2) \tag{11}$$

In order to get the total number of collisions per unit volume per unit time at a point P, Eq. (11) must be integrated over the surface elements of the body which "see" that point in space.

It is assumed that the sphere is in a uniform free-molecule flow composed of the incident molecules. The number density of this incident flow can be determined at the stagnation point of the sphere. Figure 9 shows the notation related to this part of the development. Since the flow is axially symmetric, the element of area dA in Eq. (11) may be written as

$$dA = 2\pi R^2\sin\theta d\theta \tag{12}$$

The collision density of molecules re-emitted from this area is

$$d\eta = n_w\left(\frac{2kT_w}{m\pi}\right)^{1/2}\frac{\cos\phi R^2\sin\theta}{\lambda l^2}\exp\left(\frac{-l}{\lambda}\right)d\theta \tag{13}$$

This expression must be integrated over values of θ from $\theta = 0$ to a value of θ where $\phi = \pi/2$ The total collision rate density at P is, therefore,

$$\eta = \int_{\theta=0}^{\phi=\pi/2} n_w\left(\frac{2kT_w}{\pi m}\right)^{1/2}\frac{(\cos\phi)R^2\sin\theta}{\lambda l^2}\exp\left(\frac{-l}{\lambda}\right)d\theta \tag{14}$$

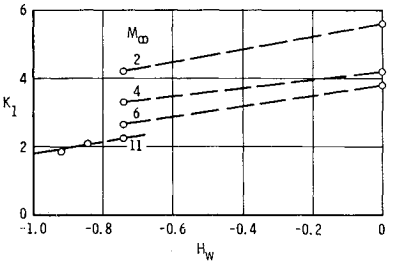

Fig. 6 Provisional values of K_1.

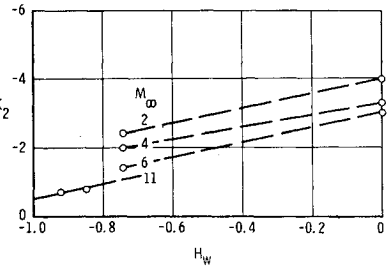

Fig. 7 Provisional values of K_2.

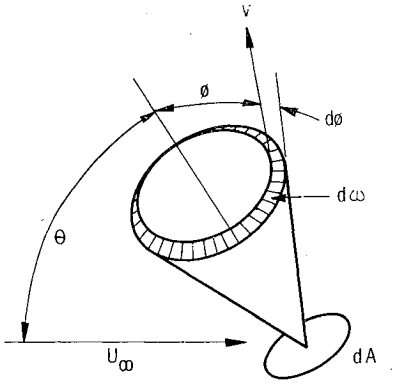

Fig. 8 Nomenclature I.

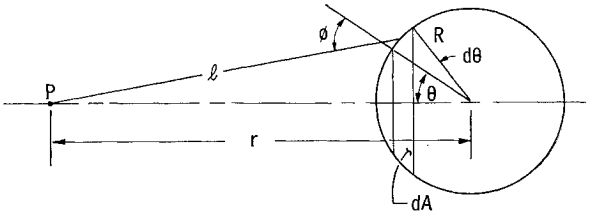

Fig. 9 Nomenclature II.

In order to evaluate this integral, it is convenient to express all variables in terms of l/λ. From the law of cosines for triangles with sides l, r, R, it is seen that

$$l^2 = r^2 + R^2 - 2rR\cos\theta \tag{15}$$

and

$$r^2 = l^2 + R^2 - 2lR(-\cos\phi) \tag{16}$$

Differentiating Eq. (15) gives

$$\sin\theta d\theta = (l/rR)dl \tag{17}$$

Let $l/\lambda = A$ when $\phi = \pi/2$ and $l/\lambda = B$ when $\theta = 0$. Note that

$$A = [(r/\lambda)^2 - (R/\lambda)^2]^{1/2} \tag{18}$$

and

$$B = r/\lambda - R/\lambda \tag{19}$$

Substituting Eqs. (9 and 15–19) into Eq. (14) gives the result

$$\eta = \frac{n_iU_\infty}{2\lambda(r/\lambda)^2(R/\lambda)}\int_B^A\left[\left(\frac{l}{\lambda}\right)^4 - 2\left(\frac{l}{\lambda}\right)^2\left(\frac{r}{\lambda}\right)^2 + \left(\frac{r}{\lambda}\right)^4 - \left(\frac{R}{\lambda}\right)^4\right]\frac{\exp(-l/\lambda)}{(l/\lambda)^2}\,d\left(\frac{l}{\lambda}\right) \tag{20}$$

Evaluating the integral in Eq. (20), one finds

$$\eta = \frac{n_iU_\infty}{2\lambda(r/\lambda)^2(R/\lambda)}\left\{e^{-B}(B^2 + 2B + 2) - e^{-A}(A^2 + 2A + 2) - 2\left(\frac{r}{\lambda}\right)^2(e^{-B} - e^{-A}) + \left[\left(\frac{r}{\lambda}\right)^4 - \left(\frac{R}{\lambda}\right)^4\right]\left[\frac{e^{-B}}{B} - [-Ei(-B)] - \frac{e^{-A}}{A} + [-Ei(-A)]\right]\right\} \tag{21}$$

Equation (21) is presented graphically in Fig. 10, where $\eta\lambda/(n_iU_\infty)$ is plotted as a function of $(r/\lambda - R/\lambda)$ for various values of R/λ.

Since the number of freestream molecules and the number of wall molecules suffering collisions are equal, the number per unit time of freestream molecules prevented from impact

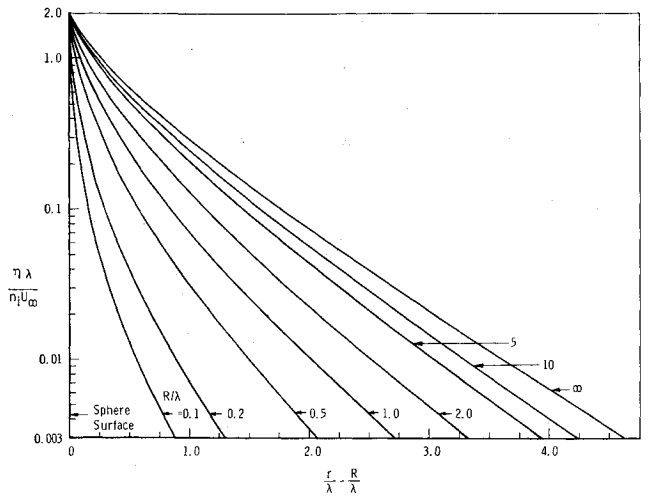

Fig. 10 Collision rate density ahead of stagnation point.

upon the sphere can be determined by integrating Eq. (21) from $l = \infty$ to the surface, $l = 0$, i.e.,

$$(n_\infty - n_i)U_\infty = \int_0^\infty \eta dl \tag{22}$$

Using Eqs. (3) and (22), it is found that

$$\frac{C_D}{C_{D_{fm}}} = \frac{1}{1 + (1/n_i U_\infty)\int_R^\infty \eta dr} = f(Kn) \tag{23}$$

The integral in Eq. (23) was evaluated numerically, using Eq. (21) for η. The result is shown in Fig. 11, where some other theories are also shown.

One of the more noteworthy aspects of Fig. 11 is the relatively close agreement of all the theories in their initial departures from the free-molecular limit. However, the several theories diverge rather rapidly at lower Knudsen numbers within the first-collision regime. It is particularly interesting to note that Eq. (23), although based on the first-collision flow model, actually approaches a limit on the order of the accepted inviscid, hypersonic flow-drag coefficient when $K_n = 0$. This happy circumstance obviously does not constitute a justification for applying first-collision concepts to the analysis of continuum flow, but it does make Eq. (23) suitable for empirical extension to form a link with the continuum regimes.

The application of any of the theories represented on Fig. 11 necessitates calculation of the mean free path of re-emitted molecules, and therein lurks an unresolved problem of kinetic theory. For example, the present authors have given a derivation[30] showing

$$\lambda = (\lambda_\infty/U_\infty)[9\pi k T_w/(4m)]^{1/2} \tag{24}$$

for fully accommodated, diffuse reflection from highly cooled, hypersonic bodies. However, not only is the question of the correct gas-surface interaction unanswered, but the true value of λ_∞ in a real gas is also a source of uncertainty in Eq. (24) and similar equations. Therefore, in order to apply Eqs. (23) and (24) to a practical case involving experimental data, it is believed excusable if the equality is replaced by a proportionality symbol, leaving a free factor to be determined by forcing agreement between Eq. (23) and the appropriate experimental data. It is interesting to express this proportionality in the form

$$Kn = \lambda/d = C\,\gamma^{1/2} M_\infty/Re_\infty \tag{25}$$

because it may be shown that $C = 2.45$ is the empirically determined factor that enables Eq. (23) to be used as a satisfactory link between the free-molecule limit and the experimental data for hypersonic, highly cooled spheres reported

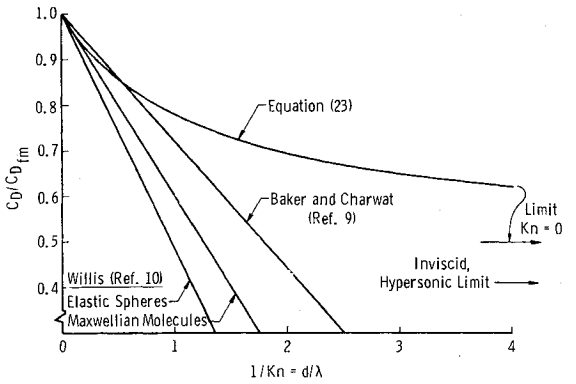

Fig. 11 Comparison of theories for the hypersonic, cold-wall, noncontinuum flow condition.

herein. In contrast, it will be noticed that Eq. (25) would be identical to the relation between Kn_∞, M_∞, and Re_∞ for a gas consisting of billiard-ball molecules if $C = 1.26$.

Equation (23), with the empirical factor from Eq. (25) used in determining $f(Kn)$, is represented in Fig. 12, where the parameter $Re_2 = Re_\infty(\mu_\infty/\mu_2)$ is chosen because it facilitates the link with Eq. (2). The value of $C_{D_{fm}}$ was computed from the equation given in Ref. 31 for fully accommodated, diffuse reflection. The purpose is to furnish a useful interpolation in an area where reliable data are not yet available.

Another theory[11] that requires use of an empirically determined factor also is represented in Fig. 12. The factor referred to as a free constant in the report by Rott and Whittenbury has been chosen by the present authors to achieve agreement with the data for lower Reynolds numbers in Fig. 12. However, it will be observed that this theory predicts a more abrupt transition from nearly inviscid to noncontinuum flows than is shown by the present data.

Conclusions

It would appear that a semiempirical approximation to the drag coefficient is capable of closely matching the experimentally determined data between the nearly inviscid, continuum and the noncontinuum flow regimes. The provisional values of the coefficients K_1 and K_2 appear to be functions of Mach number and heat transfer to the spheres in perfect gases. At Mach numbers above 6, the heat-transfer condition becomes more important than Mach number.

The first-collision type of analysis presented herein is shown to produce an equation for sphere drag coefficient which possesses several attractive features. Specifically, use of an experimentally determined factor enables the present first-collision theory to fit experimental data satisfactorily at Reynolds numbers beyond the first-collision regime. This

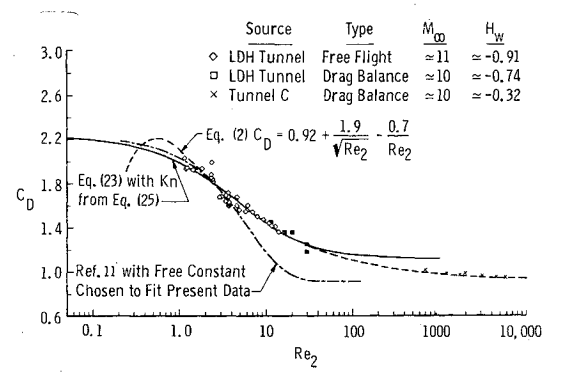

Fig. 12 Data for $M_\infty \simeq 11$ and $H_w \simeq -0.91$ compared with semiempirical analyses for continuum and noncontinuum cases.

feature makes it possible to use the theory with its empirical factor to interpolate over the gap between noncontinuum theories and available data.

References

[1] Kane, E. C., "Drag forces on spheres in low density supersonic gas flow," Univ. Calif. Rept. HE-150-65 (February 15, 1950).

[2] Sherman, F. S., "Note on sphere drag data," J. Aeronaut. Sci. **18**, 566 (1951).

[3] Jensen, N. A., "Supplementary data on sphere drag tests, Part 2," Univ. Calif. Rept. HE-150-92 (September 11, 1951).

[4] May, A , "Supersonic drag of spheres at low Reynolds numbers in free flight," J. Appl. Phys. **28**, 910–912 (1957).

[5] Masson, D. J., Morris, D. N., and Bloxsom, D. E., "Measurements of sphere drag from hypersonic continuum to free-molecule flow," Rand Corp. Res. Memo. RM-2678 (November 3, 1960).

[6] Wegener, P. P. and Ashkenas, H., "Wind tunnel measurements of sphere drag at supersonic speeds and low Reynolds numbers," J. Fluid Mech. **10**, 550–560 (1961).

[7] Potter, J. L., Kinslow, M., Arney, G. D., Jr., and Bailey, A. B., "Description and preliminary calibration of a low-density, hypervelocity wind tunnel," Arnold Eng. Dev. Center TN-61-83 (August 1961).

[8] Sreekanth, A. K., "Drag measurements on circular cylinders and spheres in the transition regime at a Mach number of 2," Univ. Toronto UTIA Rept. 74 (April 1961).

[9] Baker, R. M. L., Jr. and Charwat, A. F., "Transitional corrections to the drag of a sphere in free molecule flow," Phys. Fluids **1**, 73–81 (1958).

[10] Willis, D. R., "Study of nearly free-molecule flow," *Aerodynamics of the Upper Atmosphere*, Project Rand Rept. R-339, Paper 13 (June 1959).

[11] Rott, N. and Whittenbury, C. G., "A flow model for hypersonic rarefied gasdynamics with applications to shock structure and sphere drag," Douglas Aircraft Co. Rept. SM-38524 (May 12, 1961).

[12] Shamberg, R., "Analytical representation of surface interaction for free molecular flow with application to drag of various bodies," Rand Corp. Rept. R-339, Sec. 12 (June 1959).

[13] Chahine, M., "Similarity solution for stagnation point heat transfer in low-density, high-speed flow," Res. Summary 36-8, Jet Propulsion Lab., pp. 82–84 (May 1, 1961).

[14] Sentman, L. H., "Free molecule flow theory and its application to the determination of aerodynamic forces," Lockheed Missiles and Space Div. TR LMSD-448514 (October 1, 1961).

[15] Ashkenas, H. I., "Sphere drag at low Reynolds numbers and supersonic speeds," Res. Summary 36-12, Jet Propulsion Lab., pp. 93–95 (January 2, 1962).

[16] Aroesty, J., "Sphere drag in low density supersonic flow," Univ. Calif. Rept. HE-150-192 (January 3, 1962).

[17] Potter, J. L. and Boylan, D. E., "Experience with an overexpanded nozzle in a low-density, hypervelocity wind tunnel," Arnold Eng. Dev. Center TDR-62-85 (April 1962).

[18] Arney, G. D. Jr. and Boylan, D. E., "A calorimetric investigation of some problems associated with a low density, hypervelocity wind tunnel," Arnold Eng. Dev. Center TDR-63-19 (February 1963).

[19] Svehla, R. A., "Estimated viscosities and thermal conductivities of gases at high temperatures," NASA TR R-132 (1962).

[20] Rott, N. and Lenard, M., "Vorticity effect on the stagnation-point flow of a viscous incompressible fluid," J. Aerospace Sci. **26**, 542–543 (1959).

[21] Van Dyke, M., "Higher approximations in boundary-layer theory," Lockheed Missiles and Space Div., LMSD-703097 (October 1960).

[22] Van Dyke, M., "Second-order compressible boundary-layer theory with application to blunt bodies in hypersonic flow," *Hypersonic Flow Research*, edited by F. R. Riddell (Academic Press, Inc., New York, 1962), pp. 37–76.

[23] Cohen, C. B. and Reshotko, E., "Similar solutions for the compressible laminar boundary layer with heat transfer and pressure gradient," NACA Rept. 1293 (1956).

[24] Hodges, A. J., "The drag coefficient of very high velocity spheres," J. Aerospace Sci. **24**, 755–758 (1957).

[25] Lehnert, R., "Base pressure of spheres at supersonic speeds." U. S. Naval Ordnance Laboratory, NAVORD Rept. 2774 (February 4, 1953).

[26] Kavanau, L. H., "Base pressure studies in rarefied supersonic flows," J. Aeronaut. Sci. **23**, 193–207, 230 (1956).

[27] Schaaf, S. A. and Chambre, P. L., "Flow of rarefied gases," *Fundamentals of Gas Dynamics*, edited by H. W. Emmons (Princeton University Press, Princeton, N. J., 1958), p. 697.

[28] Kennard, E. H., *Kinetic Theory of Gases* (McGraw-Hill Book Co., Inc., New York and London, 1938), p. 62.

[29] Present, R. D., *Kinetic Theory of Gases* (McGraw-Hill Book Co., Inc., New York, Toronto, and London, 1958), p. 29.

[30] Kinslow, M. and Potter, J. L., "The drag of spheres in rarefied hypervelocity flow," Arnold Eng. Dev. Center TDR-62-205 (December 1962).

[31] Stalder, J. R. and Zurick, V. J., "Theoretical aerodynamic characteristics of bodies in a free-molecule-flow field," NACA TN-2423 (July 1951).